Pinning effects of dislocations on vortex domain structure in ferroelectric nanodots

Article *in* Applied Physics Letters · June 2014

DOI: 10.1063/1.4881884

3 authors, including:

W. J. Chen
Sun Yat-Sen University
39 PUBLICATIONS **210** CITATIONS
SEE PROFILE

Yue Zheng
National University of Singapore
81 PUBLICATIONS **713** CITATIONS
SEE PROFILE

AIP | Applied Physics Letters

Pinning effects of dislocations on vortex domain structure in ferroelectric nanodots

W. J. Chen, Yue Zheng, and Biao Wang

Citation: Applied Physics Letters **104**, 222912 (2014); doi: 10.1063/1.4881884
View online: http://dx.doi.org/10.1063/1.4881884
View Table of Contents: http://scitation.aip.org/content/aip/journal/apl/104/22?ver=pdfcov
Published by the AIP Publishing

Pinning effects of dislocations on vortex domain structure in ferroelectric nanodots

W. J. Chen,[1,2] Yue Zheng,[1,2,a)] and Biao Wang[1,b)]
[1]State Key Laboratory of Optoelectronic Materials and Technologies, Sun Yat-sen University, 510275 Guangzhou, China
[2]Micro & Nano Physics and Mechanics Research Laboratory, School of Physics and Engineering, Sun Yat-sen University, 510275 Guangzhou, China

(Received 12 April 2014; accepted 26 May 2014; published online 5 June 2014)

Effects of interfacial and internal dislocations on formation of vortex domain structure in ferroelectric nanodots have been investigated. Due to the highly inhomogeneous strain field near the dislocation core, dislocations are found to play important roles in vortex nucleation stage and can significantly affect vortex formation temperature. More importantly, the vortex core may be pinned by the dislocations, leading to a possible control of vortex domain pattern (e.g., vortices number and orientation) in the nanodots. This study should be very instructive for practical applications of ferroelectric vortex domain structure in systems where dislocations exist. © *2014 AIP Publishing LLC*. [http://dx.doi.org/10.1063/1.4881884]

Defects like dislocations, point defects, space charges, grain boundaries, cracks, etc., may be introduced into the materials during the fabrication and/or loading processes of external fields. They are well known to affect material properties by the presence of inhomogeneous mechanical and electrical fields. Take ferroelectrics as an example, defects play important roles in domain evolution processes, as they usually are favored nucleation sites of other domains.[1] Consequently, abnormal phenomena such as the reduction of coercive field,[2–4] broken degeneracy of polarization states,[5] and domain wall pining[6–8] may happen in ferroelectrics with defects. Furthermore, domain pattern, ferroelectric transition temperature, polarization, and other static properties (e.g., electrical conductance) are strongly modified near the "defective" regions.[9–14] Although it is still a long way toward "defect engineering," the revealed effects of defects in ferroelectrics during the past decades have provided us an exciting picture.

For their tunable properties and feasibility in developing nanoscale functional devices, low-dimensional ferroelectric nanostructures have been under intensive investigations. An important characteristic of these materials is the possible formation of vortex domain structure (VDS) to avoid large depolarization energy caused by surface bounded charges.[15,16] Due to the small size of ferroelectric VDS and its coupling behaviors with external fields, people are now paying much attention to this kind of domain structure. In experiment, many works aimed to unambiguously observe nanoscale ferroelectric vortices.[17–19] Meanwhile, to gain regular control of ferroelectric VDS, effects of various types of electrical and mechanical loads have been theoretically predicted.[20–25]

It is worth noting that there are quite an amount of works with respect to the effects of defects on ferroelectric domain structure. Yet, most are focused on thin films or bulk systems. The case of low-dimensional ferroelectric nanostructures has been rarely studied, although defects commonly exist in these systems.[1,10] It is natural to wonder how defects influence the VDS in these systems. As with thin films or bulk systems, we are interested in asking two questions. The first one is how defects affect VDS during its formation. Can defects act as nucleation sites of ferroelectric vortices and consequently have pining effects on the VDS? The second is how defects play their roles in the switching process of VDS. The objective of this work is to explore the first question by performing phase field simulations on the VDS in ferroelectric nanodots with different kinds of dislocations. Our model systems are schematically shown in Fig. 1. They include nanodots epitaxially grown on a substrate with an interfacial edge dislocation (Fig. 1(a)), and free standing nanodots with an edge or a screw dislocation in the body (Fig. 1(b)).

In phase field models, the evolution of a microstructure is driven by the decrease of the system's free energy. We take the unstressed and unpolarized crystal as the background and express the system's free energy in terms of order parameters and applied fields. The spontaneous polarization $\mathbf{P} = (P_1, P_2, P_3)$ is chosen as the order parameter. The electric displacement field $\mathbf{D}$ is written as $\mathbf{D} = \boldsymbol{\varepsilon}_\mathbf{b}\mathbf{E} + \mathbf{P}$, with $\mathbf{E}$ being the electric field and $\boldsymbol{\varepsilon}_\mathbf{b}$ being the background dielectric constant tensor.[26,27] The system's total free energy is written as a sum of the bulk Landau energy, elastic energy, gradient energy, electrostatic energy, and surface energy, i.e., $F = \int_V (f_{\text{Land}} + f_{\text{elas}} + f_{\text{grad}} + f_{\text{elec}})dV + \int_S f_{\text{surf}} dS$, where V and S are the volume and surface of the system, respectively.

In equation of the total free energy, the Landau energy density f_{Land}, which describes the ferroelectric transition of the bulk material, can be written as a six-order phenomenological polynomial of the spontaneous polarization, i.e.,[28,29] $f_{\text{Land}} = a_1\sum_i P_i^2 + a_{11}\sum_i P_i^4 + a_{12}\sum_{i>j} P_i^2P_j^2 + a_{111}\sum_i P_i^6 + a_{112}\sum_{i>j}(P_i^4P_j^2 + P_j^4P_i^2) + a_{123}\prod_i P_i^2$, where a_1, a_{11}, a_{12}, a_{111}, a_{112}, and a_{123} are phenomenological coefficients, with

a)Author to whom correspondence should be addressed. Electronic mail: zhengy35@mail.sysu.edu.cn
b)Electronic mail: wangbiao@mail.sysu.edu.cn

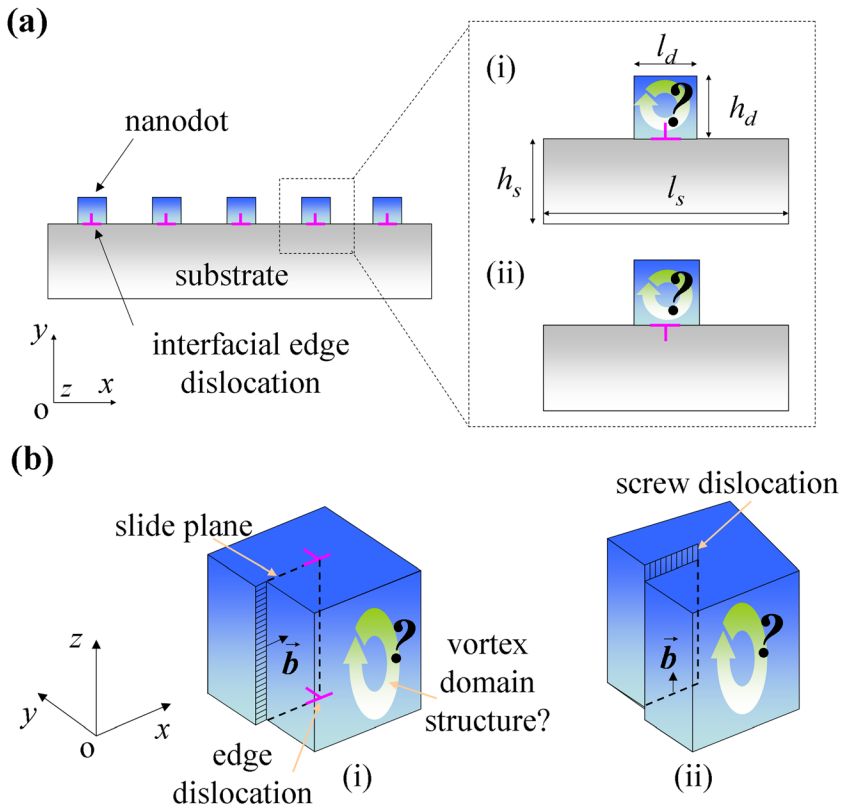

FIG. 1. Schematics of the model systems. (a) Epitaxial ferroelectric nanodots with an edge dislocation at the substrate-nanodot interface. (b) Free standing ferroelectric nanodots with an internal edge dislocation or a screw dislocation line.

a_1 linearly dependent on temperature and obeying the Curie–Weiss law.

Based on the theory of micromechanics,[30] ferroelectric domains and dislocations are treated as sources of eigenstrains. The eigenstrain generated by the polarization is given by $\varepsilon_{ij}^{0,P} = Q_{ijkl}P_kP_l$, with Q_{ijkl} being the fourth-rank electrostrictive coefficients. The dislocation line is defined as a part of a slip plane. The eigenstrain related to a dislocation on a slip plane with a Burgers vector $\mathbf{b}^s = (b_1^s, b_2^s, b_3^s)$ is described as $\varepsilon_{ij}^{0,D}(\mathbf{x}) = \frac{1}{2}(b_i^s n_j^s + b_j^s n_i^s)\delta(\mathbf{x} - \mathbf{x}_0^s)/d_0$,[3,9] where $\mathbf{n}^s = (n_1^s, n_2^s, n_3^s)$ is the unit vector normal to the slip plane, d_0 is the interplanar distance of the slip planes, and $\delta(\mathbf{x} - \mathbf{x}_0^s)$ is the Dirac delta function with $\mathbf{x}_0^s$ being a point on the slip plane. The incompatibility of these eigenstrains and the application of external force or constraint would cause an elastic energy f_{elas}, as described by $f_{\text{elas}} = \frac{1}{2}c_{ijkl}e_{ij}e_{kl} = \frac{1}{2}c_{ijkl}(\varepsilon_{ij} - \varepsilon_{ij}^{0,P} - \varepsilon_{ij}^{0,D})(\varepsilon_{kl} - \varepsilon_{kl}^{0,P} - \varepsilon_{kl}^{0,D})$, with c_{ijkl} being the fourth-rank elastic stiffness coefficients, and e_{ij} and ε_{ij} being the components of elastic strain and total strain, respectively. The strain field is determined by the mechanical equilibrium equation, i.e., $\sigma_{ij,j} = 0$, where $\sigma_{ij} = c_{ijkl}e_{kl}$ is the stress components.

The inhomogeneous polarization field contributes a gradient energy to the system's free energy. To the lowest order of Taylor expansion, the gradient energy density takes the form as $f_{\text{grad}} = \frac{1}{2}g_{ijkl}P_{i,j}P_{k,l}$, with g_{ijkl} being gradient energy coefficients. Moreover, electrostatic energy should be considered due to Coulomb interaction of polarization dipoles. According to the continuum theory, the electric energy density of the system is written as $f_{\text{elec}} = -P_iE_i - \frac{1}{2}\varepsilon_b E_iE_i$.[26,31] For a free-charge-absent body, the electric field can be calculated by the electrostatic equilibrium equation as $D_{i,i} = 0$. Using the so-called extrapolation length δ_i^{eff},[32,33] an additional surface energy is introduced to describe the intrinsic polarization inhomogeneity across the surfaces, i.e., $f_{\text{surf}} = \frac{1}{2}D_i^s P_i^2/\delta_i^{\text{eff}}$, with D_i^s being the material coefficients related to the gradient energy coefficients and surface orientation.

The temporal evolution of the spontaneous polarization field is described by the time-dependent Ginzburg–Landau (TDGL) equation $\partial P_i/\partial t = -M\delta F/\delta P_i$, where M is a kinetic coefficient and t is time. In the present study, we focus on the domain structure of (001) oriented $PbTiO_3$ nanodots upon a cooling-down process. For epitaxial nanodots in Fig. 1(a), two types of interfacial edge dislocation lines parallel to the z-axis are considered. They are c_{I} dislocation with $\mathbf{b}^s = b_0(1, 0, 0)$ and c_{II} dislocation with $\mathbf{b}^s = b_0(-1, 0, 0)$, respectively. The simulation cell is chosen to include the nanodot and a sufficient large region of substrate. A periodic boundary condition is imposed to the simulation cell along the x direction. A two-dimensional (2D) discrete grid is employed with the element size being $\Delta x = \Delta y = 1$nm. Note that the effect of grid size has been checked by conducting some of the simulations on a finer grid and the obtained domain patterns are found similar (see supplementary material[34]). The width and the height of the nanodots are l_{d} and h_{d}, and those of the substrate region are fixed as $l_{\text{s}} = 100$ nm and $h_{\text{s}} = 40$ nm. For free standing nanodots in Fig. 1(b), we consider both edge and screw dislocations. The dislocation lines are parallel to the z-axis and across the center of nanodot. A three-dimensional (3D) simulation cell is employed. The size of the nanodots are $20\,\text{nm} \times 20\,\text{nm} \times 20\,\text{nm}$ with the element size being $\Delta x = \Delta y = \Delta z = 1$nm. To explore the possible formation of VDS, an open-circuit condition is considered by setting $D_\perp = 0$ at the surfaces of the nanodot, with $D_\perp$ being the component of electric displacement perpendicular to the surface. The free surfaces of the nanodot are assumed to be traction-free.

The polarization evolution is solved numerically by discretizing the TDGL equation in time. At each time step, the strain and electric fields are obtained by solving the mechanical and electrostatic equilibrium equations with the appropriate boundary conditions. A finite element method is adopted to solve the strain and electric fields.[24] Coefficients of ferroelectric materials and dislocations in our simulations are listed in Ref. 35.[9,26,29,33,36] The distribution of mechanical field in epitaxial and free standing nanodots have been calculated, and are given in supplementary material.[34]

The formation of VDS and its evolution of three epitaxial nanodots (i.e., one free of dislocation, one with c_{I} dislocation, and one with c_{II} dislocation) under a cooling-down process are simulated. The size of the nanodots is $l_{\mathrm{d}} = h_{\mathrm{d}} = 20\,\mathrm{nm}$. The nanodots are cooled down from a high temperature at paraelectric region by a step of 10 K. A random polarization perturbation is used to initiate the simulation at high temperature until the nanodot is not in paraelectric phase. At each temperature, the stable domain pattern is obtained by equilibrating the system for a sufficiently long time. The result is depicted in Fig. 2, from which we find that the interfacial dislocations have strong effect on the formation of VDS in the nanodot. As indicated by the evolution of toroidal moment (i.e., $\mathbf{g} = \frac{1}{V}\int_V \mathbf{r} \times \mathbf{P} dV$) in Fig. 2(a), a paraelectric to ferrotoroidic transition happens when the temperature decreases to be about 710 K for the nanodot free of dislocation. Such a transition temperature is lower than the bulk Curie temperature (~752 K) as expected, considering the finite size effect of the nanodot and the small clamping effect of substrate (as we have assumed a zero misfit strain). Nevertheless, the domain patterns of the nanodot at $T = 700\,\mathrm{K}$, 500 K, and 300 K shown in panel (i) of Fig. 2(b) indicate that the substrate actually leads to a slight asymmetry of the domain pattern along the thickness direction, and this effect becomes more significant at lower temperature. This is due to the fact that the vortex domain pattern has an "eigenstrain," which is incompatible with the substrate and increases as the temperature decreases.

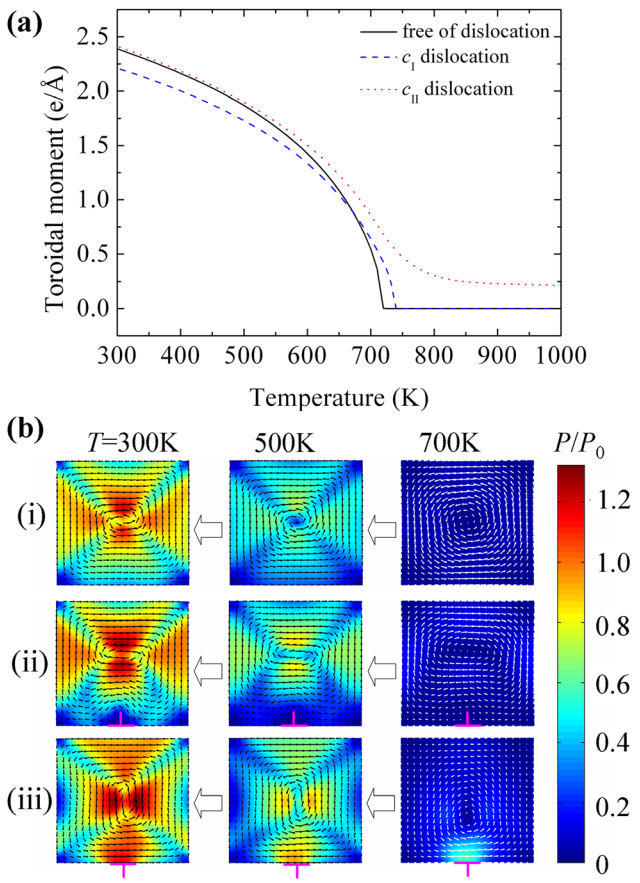

FIG. 2. Evolution of the domain pattern of three epitaxial nanodots, i.e., one free of dislocation, one with c_{I} dislocation, and one with c_{II} dislocation. The size of the nanodots are $l_{\mathrm{d}} = h_{\mathrm{d}} = 20\,\mathrm{nm}$. (a) Toroidal moment as a function of temperature and (b) domain patterns of the three nanodots at selected temperatures.

For nanodots with an interfacial dislocation, from Fig. 2, we can see that the nanodots still adopt VDS. Nevertheless, the effects of the dislocations are clearly seen. Specifically, the existence of c_{I} dislocation increases the ferrotoroidic transition temperature to be ~730 K. Upon the cooling-down process, the increase of the toroidal moment of the nanodot with c_{I} dislocation is slower than that without dislocation (Fig. 2(a)). Moreover, as shown in panel (ii) of Fig. 2(b), the domain pattern near the interface is perturbed by the inhomogeneous but overall compressive strain field of c_{I} dislocation,[34] leading to a "dead layer" of polarization field similar to that observed in ferroelectric thin films.[12,13] On the other hand, we found that c_{II} dislocation significantly increases the ferrotoroidic transition temperature of the nanodot, manifested with a nonzero toroidal moment at temperature over 1000 K. For this case, evolution of the toroidal moment consists of two distinct stages. At high temperature region, the toroidal moment remains small and increases slowly as temperature decreases. As the temperature reaches a transition point of ~750 K, the toroidal moment grows rapidly in a similar trend with that of the nanodot free of dislocation (see Fig. 2(a)). From the domain patterns as shown in panel (iii) of Fig. 2(b), we can see that there is actually a large polarization field along the x direction near the c_{II} dislocation as it imposes a large tensile strain field.[34] As this tensile strain field is highly localized, the polarization vortex formed near the c_{II} dislocation at high temperature is highly asymmetric with the polarization magnitude decreasing rapidly away from the dislocation.

From the previous simulation, it can be noticed that polarization vortex tends to nucleate around the c_{II} dislocation as it provides a localized tensile strain field. In other words, there may be a vortex pinning effect of the dislocation. For nanodots that favor a multi-vortex domain pattern rather than a single-vortex domain pattern, this effect should be significant and leads to a possible control of the vortices number. To see this, we simulate the domain formation of two epitaxial nanodots in larger size (i.e., $h_{\mathrm{d}} = 20\,\mathrm{nm}$ and $l_{\mathrm{d}} = 40\,\mathrm{nm}$) upon a cooling-down process. One of the nanodots is free of dislocation while the other one is with a c_{II} dislocation at the center of the interface. Moreover, an external strain of $\varepsilon_{11}^{\mathbf{a}} = -0.01$ is applied to the nanodots so that a multi-vortex domain pattern is favored to form. The simulation result is shown in Fig. 3. For the nanodot free of dislocation (see Fig. 3(b)), a 4-vortices domain pattern is formed during the cooling-down process. The nucleation of vortices is rather "homogenous," and the vortices grow in a similar speed. However, the situation is quite different for the

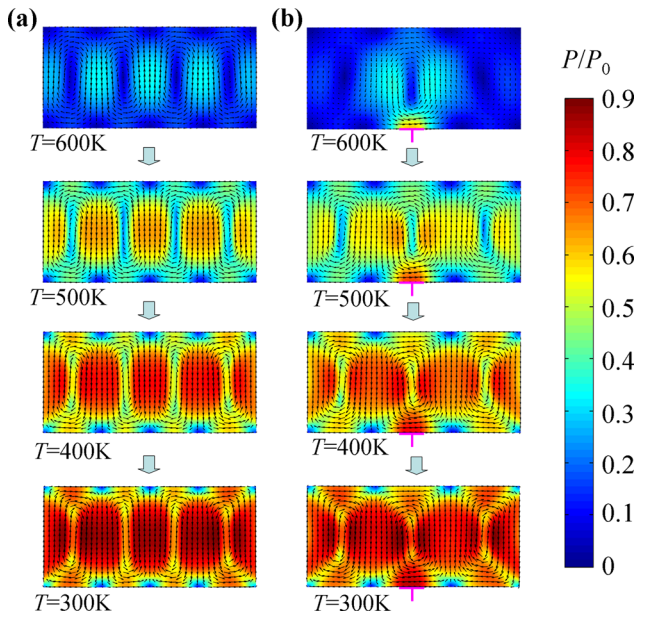

FIG. 3. Domain pattern evolution of two epitaxial nanodots ($h_d = 20$ nm and $l_d = 40$ nm) upon a cooling-down process. One of the nanodots is (a) free of dislocation and (b) the other one is with a c_{II} dislocation at the center of the interface. An external strain of $\bar{\varepsilon}^a_{11} = -0.01$ is applied to the nanodots.

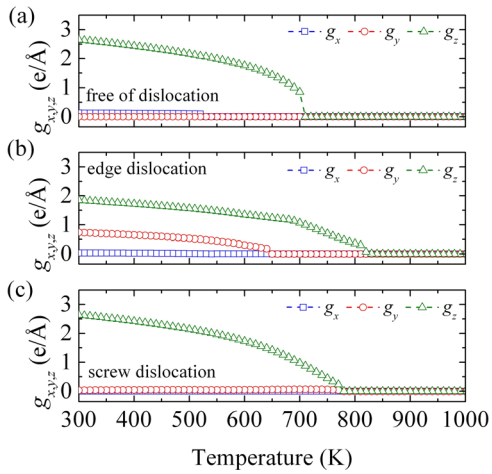

FIG. 4. Evolution of the toroidal moment of three free standing nanodots of size 20 nm × 20 nm × 20 nm upon a cooling-down process. (a) A nanodot free of dislocation, (b) a nanodot with an internal edge dislocation, and (c) a nanodot with an internal screw dislocation. The dislocation lines are parallel with z-axis and across the center of nanodot.

nanodot with a c_{II} dislocation. The nucleation of vortices is quite "inhomogeneous" due to the dislocation as shown in Fig. 3(b). A vortex would first nucleate and grow around the dislocation. Due to the existence of this vortex, there only two other nucleation sites are favored to form in the adjacent regions near the dislocation. Consequently, a 3-vortices domain pattern is formed. This result clearly demonstrates the important role of dislocation in the formation of VDS.

We now turn to the case of free standing nanodots with an internal edge or screw dislocation as schematically shown in Fig. 1(b). Similar with the previous investigation, three nanodots, i.e., one free of dislocation, one with an edge dislocation, and one with a screw dislocation,[34] are simulated under a cooling-down process. Evolution of the toroidal moment of three nanodots is, respectively, depicted in Figs. 4(a)–4(c). In Fig. 5, we also depict the domain patterns of the nanodots at two typical temperatures, i.e., $T = 700$ K and $T = 300$ K. Fig. 4(a) shows that the ferrotoroidic transition temperature of the nanodot free of dislocation is about 710 K, which is similar to that of the epitaxial nanodot free of dislocation (see Fig. 2). The existence of an edge dislocation and a screw dislocation increases the transition temperature to be about 820 K and 780 K, respectively. All the nanodots are found to first exhibit a tetragonal vortex domain pattern (i.e., with only one nonzero component of the toroidal moment) upon the cooling-down process. Nevertheless, different from the nanodot free of dislocation and the one with a screw dislocation, the nanodot with an edge dislocation adopts a vortex domain pattern with two nonzero components as the temperature is lower than 650 K (see Fig. 4(b)). From Figs. 5(a) and 5(c), we can see that the nanodot free of dislocation and the one with a screw dislocation form similar single-vortex domain patterns, with the latter one "distorted" from the former one due to the high strain field near the screw dislocation. For the nanodot with an edge dislocation, a single-vortex domain pattern would be formed at

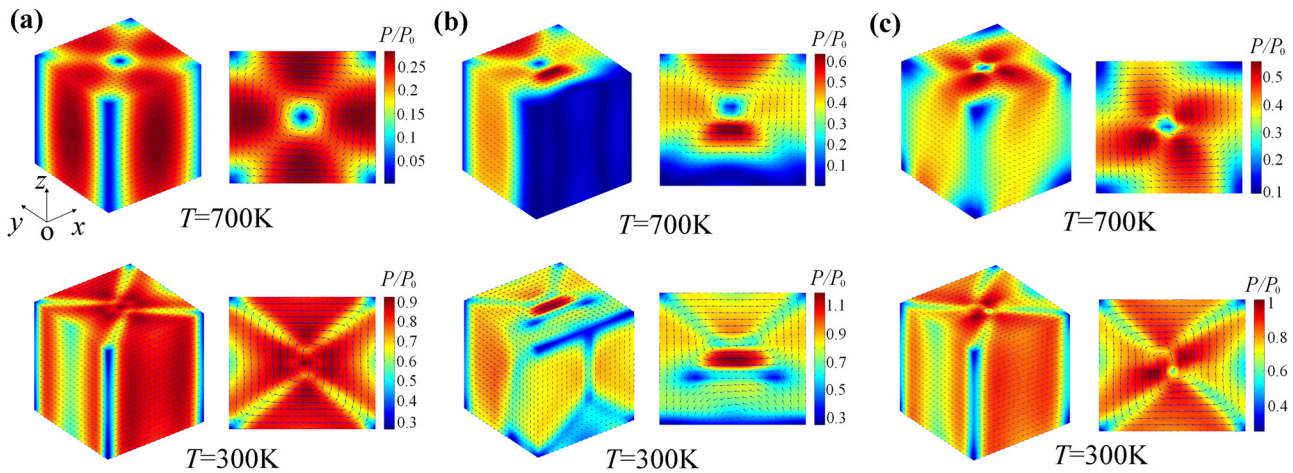

FIG. 5. Domain patterns of three free standing nanodots of size 20 nm × 20 nm × 20 nm upon a cooling-down process at two typical temperatures, i.e., $T = 700$ K and $T = 300$ K. (a) A nanodot free of dislocation, (b) a nanodot with an internal edge dislocation, and (c) a nanodot with an internal screw dislocation. The dislocation lines are parallel with z-axis and across the center of nanodot.

high temperature, and a multi-vortex domain pattern is formed at low temperature (Fig. 5(b)). Moreover, it should be pointed out that the tetragonal vortex domain pattern of the perfect nanodot is actually degenerated in x, y, and z direction. In contrast, for nanodots with an edge or screw dislocation, the degeneration of x, y, and z direction is broken. Using different random polarization perturbations to initiate the simulation, we found that the domain patterns of the two nanodots always have the largest toroidal moment component along the z direction. In other words, the orientation of the vortex domain pattern is pinned by the dislocations, and the vortex axis is along the z direction. This interesting result provides us an insight into the control of vortex orientation by inhomogeneous mechanical field in addition to previous reported strategy by uniform strain field.[25]

In summary, in this Letter we report the effects of interfacial and internal dislocations on the VDS in ferroelectric nanodots. Our calculations show that dislocations can significantly affect the formation of VDS, and play important roles in the vortex nucleation stage due to the high strain field near the dislocation core. Consequently, the vortex formation temperature of the nanodot can be significantly affected by the existence of dislocations. Importantly, the vortex core can be pinned by the dislocations, leading to a possible control of vortices number and orientation in the nanodots. Our results are important for applications of ferroelectric VDS. Note that the dislocations should have important effects on the switching process of VDS. We would like to make an investigation on this issue in a future work.

The authors acknowledge the financial support of the National Natural Science Foundation of China (NSFC) (Nos. 51172291, 11232015, and 11372361). Yue Zheng also thanks support by the Fundamental Research Funds for the Central Universities, NCET in University, Research Fund for the Doctoral Program of Higher Education, Fok Ying Tung Foundation, Science and Technology Innovation Project of Guangdong Provincial Education Department, and Guangdong Natural Science Funds for Distinguished Young Scholar.

[1]S. V. Kalinin, B. J. Rodriguez, A. Y. Borisevich, A. P. Baddorf, N. Balke, H. J. Chang, L.-Q. Chen, S. Choudhury, S. Jesse, P. Maksymovych, M. P. Nikiforov, and S. J. Pennycook, Adv. Mater. **22**, 314 (2010).
[2]R. Ahluwalia and W. Cao, Phys. Rev. B **63**, 012103 (2000).
[3]Y. L. Li, S. Y. Hu, S. Choudhury, M. I. Baskes, A. Saxena, T. Lookman, Q. X. Jia, D. G. Schlom, and L. Q. Chen, J. Appl. Phys. **104**, 104110 (2008).
[4]H. H. Wu, J. Wang, S. G. Cao, and T. Y. Zhang, Appl. Phys. Lett. **102**, 232904 (2013).
[5]P. Maksymovych, N. Balke, S. Jesse, M. Huijben, R. Ramesh, A. P. Baddorf, and S. V. Kalinin, J. Mater. Sci. **44**, 5095 (2009).
[6]W. Zhang and K. Bhattacharya, Acta Mater. **53**, 199 (2005).
[7]P. Gao, C. T. Nelson, J. R. Jokisaari, S.-H. Baek, C. W. Bark, Y. Zhang, E. Wang, D. G. Schlom, C.-B. Eom, and X. Pan, Nat. Commun. **2**, 591 (2011).
[8]A. Kontsos and C. M. Landis, Int. J. Solids Struct. **46**, 1491 (2009).
[9]S. Y. Hu, Y. L. Li, and L. Q. Chen, J. Appl. Phys. **94**, 2542 (2003).
[10]M. W. Chu, I. Szafraniak, R. Scholz, C. Harnagea, D. Hesse, M. Alexe, and U. Gosele, Nat. Mater. **87**, 3 (2004).
[11]J. M. Wesselinowa, S. Trimper, and K. Zabrocki, J. Phys.: Condens. Matter **17**, 4687 (2005).
[12]Y. Zheng, B. Wang, and C. H. Woo, Appl. Phys. Lett. **88**, 092903 (2006).
[13]Y. Zheng, B. Wang, and C. H. Woo, J. Mech. Phys. Solids **55**, 1661 (2007).
[14]D. Lee, S. M. Yang, J.-G. Yoon, and T. W. Noh, Nano Lett. **12**, 6436 (2012).
[15]H. Fu and L. Bellaiche, Phys. Rev. Lett. **91**, 257601 (2003).
[16]I. I. Naumov, L. Bellaiche, and H. Fu, Nature **432**, 737 (2004).
[17]B. J. Rodriguez, X. S. Gao, L. F. Liu, W. Lee, I. I. Naumov, A. M. Bratkovsky, D. Hesse, and M. Alexe, Nano Lett. **9**, 1127 (2009).
[18]A. Schilling, D. Byrne, G. Catalan, K. G. Webber, Y. A. Genenko, G. S. Wu, J. F. Scott, and J. M. Gregg, Nano Lett. **9**, 3359 (2009).
[19]L. J. McGilly and J. M. Gregg, Nano Lett. **11**, 4490 (2011).
[20]S. Prosandeev, I. Ponomareva, I. Kornev, I. Naumov, and L. Bellaiche, Phys. Rev. Lett. **96**, 237601 (2006).
[21]S. Prosandeev, I. Ponomareva, I. Kornev, and L. Bellaiche, Phys. Rev. Lett. **100**, 047201 (2008).
[22]I. Naumov and H. Fu, Phys. Rev. Lett. **98**, 077603 (2007); Phys. Rev. Lett. **101**, 197601 (2008).
[23]J. Wang and M. Kamlah, Phys. Rev. B **80**, 012101 (2009).
[24]W. J. Chen, Y. Zheng, and B. Wang, Appl. Phys. Lett. **100**, 062901 (2012); W. J. Chen, Y. Zheng, and B. Wang, Sci. Rep. **2**, 796 (2012).
[25]W. J. Chen, Y. Zheng, B. Wang, D. C. Ma, and F. R. Ling, Phys. Chem. Chem. Phys. **15**, 7277 (2013).
[26]Y. Zheng and C. H. Woo, Appl. Phys. A: Mater. Sci. Process. **97**, 617 (2009); C. H. Woo and Y. Zheng, Appl. Phys. A: Mater. Sci. Process. **91**, 59 (2008).
[27]A. K. Tagantsev, Ferroelectrics **375**, 19 (2008).
[28]M. J. Haun, E. Furman, S. J. Jang, H. A. McKinstry, and L. E. Cross, J. Appl. Phys. **62**, 3331 (1987).
[29]N. A. Pertsev, A. G. Zembilgotov, and A. K. Tagantsev, Phys. Rev. Lett. **80**, 1988 (1998).
[30]T. Mura, *Micromechanics of Defects in Solids* (Martinus Nijhoff Publishers, Dordrecht, 1987).
[31]L. D. Landau, E. M. Lifshitz, and L. P. Pitaevskii, *Electrodynamics of Continuous Media* (Oxford University Press, Oxford, 1984).
[32]R. Kretschmer and K. Binder, Phys. Rev. B **20**, 1065 (1979).
[33]K. Ishikawa and T. Uemori, Phys. Rev. B **60**, 11841 (1999).
[34]See supplementary material at http://dx.doi.org/10.1063/1.4881884 for the additional results on grid size effect and distribution of mechanical field.
[35]Values of parameters in calculation (SI units): $a_1 = 3.85(T - 752) \times 10^5$, $a_{11} = -7.3 \times 10^7$, $a_{12} = 7.5 \times 10^8$, $a_{111} = 2.6 \times 10^8$, $a_{112} = 6.1 \times 10^8$, $a_{123} = -3.7 \times 10^9$, $c_{11} = 1.746 \times 10^{11}$, $c_{12} = 0.7937 \times 10^{11}$, $c_{44} = 1.1111 \times 10^{11}$, $Q_{11} = 0.089$, $Q_{12} = -0.026$, $Q_{44} = 0.0675$, $G_{11} = 2G_{44} = 2G'_{44} = 2G_{110}$, $G_{110} = 1.73 \times 10^{-10}$, $\delta_i^{\text{eff}} = 5 \times 10^{-9}$, $\varepsilon_b = 4.425 \times 10^{-10}$, $d_0 = 4 \times 10^{-10}$, $b_0 = d_0/3$, and $P_0 = 0.757$.
[36]Y. L. Li, S. Y. Hu, Z. K. Liu, and L. Q. Chen, Appl. Phys. Lett. **81**, 427 (2002).